

# VIBRATION-POWERED BATTERY-LESS SENSOR NODE USING MEMS ELECTRET GENERATOR

Koichi Matsumoto<sup>1</sup>, Kumio Saruwatari<sup>2</sup>, and Yuji Suzuki<sup>1\*</sup>

<sup>1</sup>Department of Mechanical Engineering, The University of Tokyo, Tokyo, Japan

<sup>2</sup>TechnoDesign Co., Ltd, Kumamoto, Japan

\*Presenting Author: ysuzuki@mesl.t.u-tokyo.ac.jp

**Abstract:** Battery-less wireless sensor node using a vibration-driven MEMS electret energy harvester has been prototyped. With non-linear parylene springs and high-performance electret material based on fluorinated polymer CYTOP, more than 3  $\mu\text{W}$  power output is obtained in a broad range vibration frequency of 26-40 Hz at 1.4 G. By integrating the energy harvester with a power management circuit, low-power-consumption CPU, and RFIC, intermittent wireless transmission with an interval of 80.6 s has been realized.

**Keywords:** Energy harvesting, MEMS, electret, Sensor network node

## INTRODUCTION

Energy harvesting from environmental vibration attracts much attention for its use in battery-less wireless sensor network nodes [1-4]. Such system can be used in various applications such as home/building energy management systems (HEMS/BEMS) and structural health monitoring systems. Since the frequency range of environmental vibration is tens of hertz, electrostatic power generators using electret should have higher performance than the other energy conversion principles [5-11]. In our previous studies, we have developed a novel high-performance polymer electret material based on CYTOP (Asahi Glass) [7, 12] and a new MEMS fabrication process for high-aspect-ratio polymer springs [13, 14], and obtained 1  $\mu\text{W}$  power output at 63 Hz and 2 G with our early prototype generator.

In the present study, we microfabricate a MEMS electret energy harvester prototype with an improved electrode design and develop a battery-less wireless sensor node by integrating the electret generator with a power management circuit, a CPU and a RFIC.

## MEMS ELECTRET GENERATOR

The outline of the present electret generator is schematically shown in Fig. 1. In response to the in-plane oscillation of the mass supported with the polymer springs, the overlapping area of the electret and the counter electrode is changed, producing an AC current in the external circuit due to the change in the amount of the induced charges.

We employed aminosilane-doped CYTOP [7, 12] as the electret material to achieve high surface charge density. Kashiwagi et al. [12] recently reported that nano clusters are formed by the condensation reaction among aminosilane molecules in the CYTOP film, which serve as the localized charge traps. Using this electret film with 15  $\mu\text{m}$  in thickness, an extremely-high surface charge density of 2  $\text{mC}/\text{m}^2$  as well as higher thermal stability of charges can be obtained.

In order to capture low-frequency vibration and convert it into large-amplitude oscillation of the Si

mass, the mass is supported with four parylene high-aspect-ratio springs [13], of which spring constant is as low as 10 N/m. Fixed-free secondary springs, of which spring constant is 20 N/m, are also formed on both sides of the Si frame in order to realize nonlinear response of the spring for broadening the operating frequency range [15]. Electrostatic repulsive force between patterned electrets [14] is employed to keep the narrow gap between the top and the bottom electrodes. Micro beads 50  $\mu\text{m}$  in diameter are also introduced between the electrodes to avoid accidental stiction during seismic operation.

In addition, a new design of the dual-phase arrangement of electrodes is employed in order to reduce the magnitude of unidirectional horizontal electrostatic force [14]. In the present study, electrodes of different phases are separated in the direction normal to the oscillation direction, which minimize unbalance of the electrostatic force in the oscillation direction.

## FABRICATION PROCESS

Figure 2 shows the process flow of the MEMS electret generator. For the top substrate with a seismic mass, 20- $\mu\text{m}$ -wide 350- $\mu\text{m}$ -deep trenches are etched into a Si substrate using thermal oxide as the etching

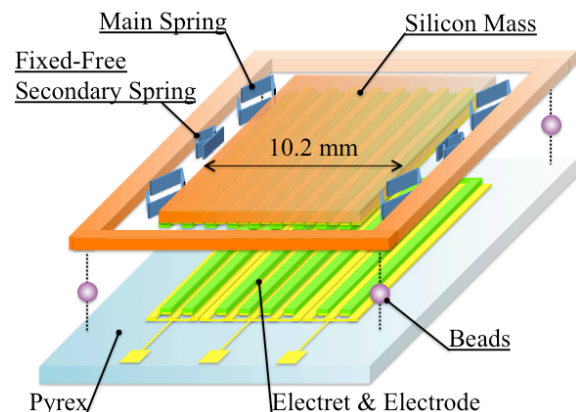


Figure 1 Overall design of in-plane MEMS electret generator.

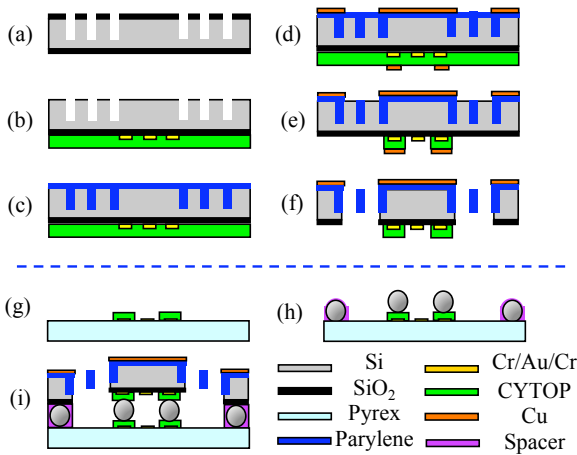


Figure 2. MEMS process of the electret generator.

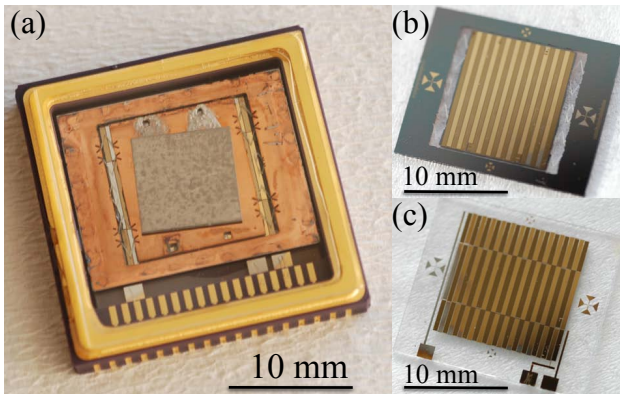


Figure 3. Overview of the electret generator. (a) Prototype packaged in a ceramic case, (b) Top Si substrate, and (c) Bottom glass substrate.

mask (Fig. 2a). Then, bottom Cr/Au/Cr electrodes and 15- $\mu\text{m}$ -thick CYTOP films are patterned (Fig. 2b). Next, 15- $\mu\text{m}$ -thick parylene-C is deposited on the front side and etched back with  $\text{O}_2$  plasma. This is followed by the second parylene-C deposition to fully refill the trenches (Fig. 2c). The parylene and CYTOP films are patterned with  $\text{O}_2$  plasma (Fig. 2de) using a metal hard mask. Finally, the Si substrate used as the parylene molds is etched away with  $\text{XeF}_2$ , and the structures are released (Fig. 2f). For the bottom Pyrex substrate, Cr/Au/Cr electrodes and CYTOP film are patterned (Fig. 2g). Finally, the CYTOP electrets are corona charged, and the top Si substrate and the bottom Pyrex substrate are aligned and bonded (Fig. 2hi). The air gap between the substrates is 50  $\mu\text{m}$ . Width of the electrode/electrets is 480  $\mu\text{m}$ . Initial surface potential of the electret film is -760 ~ -800 V.

Figure 3 shows photos of the generator prototype presently developed. As shown in Fig. 3c, the bottom electrodes are divided into two separate phases, i.e., the center and the side phases. Contact pads on the glass substrate correspond to the common ground and the output of the two phases. After assembling the top Si substrate and the bottom glass substrate using a bond aligner, the device is packaged in a ceramic case filled with  $\text{SF}_6$  gas to suppress possible discharge between the air gap.

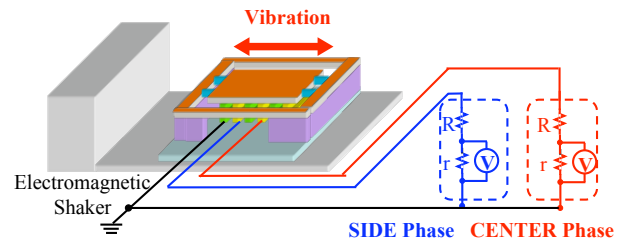


Figure 4. Experimental setup.

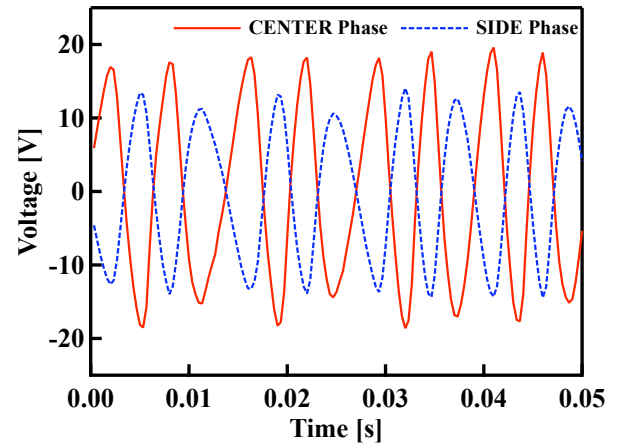


Figure 5. Time trace of the output voltage at 40 Hz and 1.4 G.

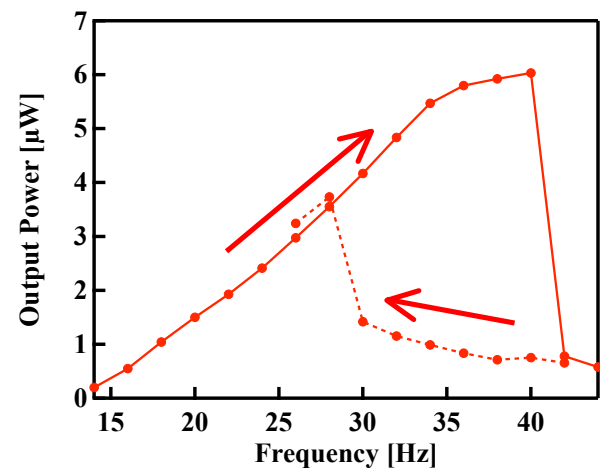


Figure 6. Output power at 1.4 G for different frequencies.

## POWER GENERATION EXPERIMENT

Power generation performance of the MEMS generator is examined with a setup shown in Fig. 4. The generator is fixed on an electromagnetic shaker (ET-141, Labworks), and oscillated in the in-plane direction. Each phase of the generator is connected to a separate external load. Parasitic capacitance of the present device is 12 pF. Optimum load for the matched impedance is found to be 40  $\text{M}\Omega$ .

Figure 5 shows the output voltage at 40 Hz and 1.4 G acceleration. Under this experimental condition, amplitude of the mass is about 2  $\text{mm}_{\text{p-p}}$ . AC outputs with peak-to-peak voltage of 36 V and 28 V are obtained for the center and the side phases, respectively. The voltage signals are 180-degree out-of-phase as designed. Figure 6 shows the output power versus frequency at a constant acceleration of 1.4 G. Maximum power output of 6  $\mu\text{W}$  is obtained at 40 Hz,

which is six times larger than our previous data [14]. Thanks to the nonlinear springs, power output more than  $3 \mu\text{W}$  has been obtained in a broad frequency range of 26-40 Hz, when the frequency is increased from 20 Hz. On the other hand, when the frequency is decreased from 40 Hz, the power output takes the lower branch, showing the hysteresis of the power output.

Figures 7 and 8 show the power spectra of a pseudo environmental vibration with  $1.2 G_{\text{rms}}$  acceleration and the output voltage, respectively. It is found that even for random vibration with a broad spectrum, mean power output of  $3.4 \mu\text{W}$  has been obtained.

### DEVELOPMENT OF A WIRELESS NETWORK NODE PROTOTYPE

An early prototype of a wireless sensor node, which consists of the electret generator, a power management circuit, a low-power-consumption CPU (MSP430 F2618, Texas Instruments), and a wireless IC (nRF24L01, Nordic Semiconductor), is developed. Figure 9 shows the circuit diagram. The two voltage outputs from the generator are rectified by a pair of bridge diodes and the charge is accumulated in a common capacitor. When the capacitor voltage reaches 4.9 V, the charge controller initiates the discharge with

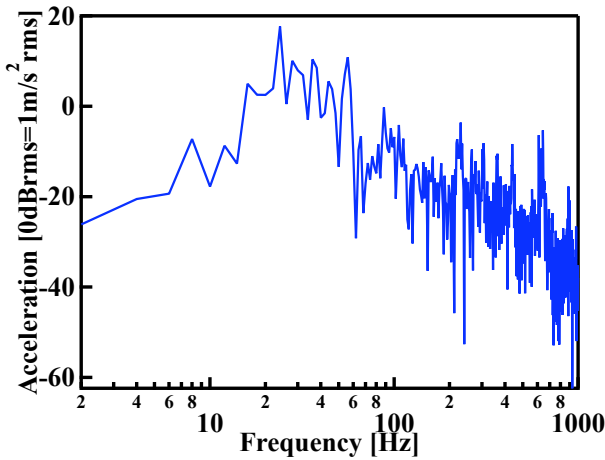


Figure 7. Power spectrum of the pseudo environmental vibration.

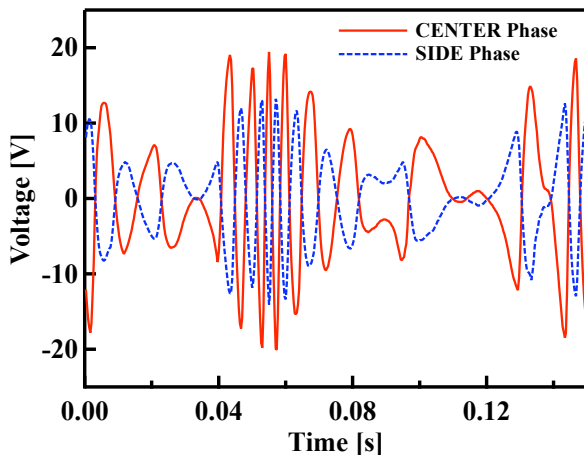


Figure 8. Time trace of the output voltage for the pseudo environmental vibration.

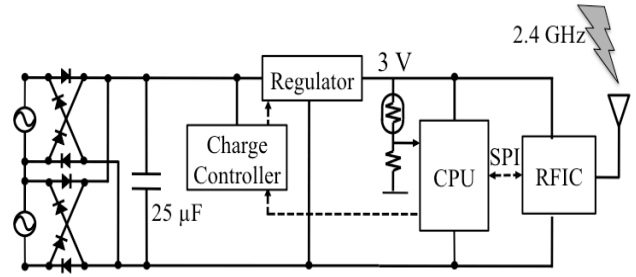


Figure 9. An early prototype of wireless network node integrated with the electret generator, a power management circuit, CPU and RFIC.

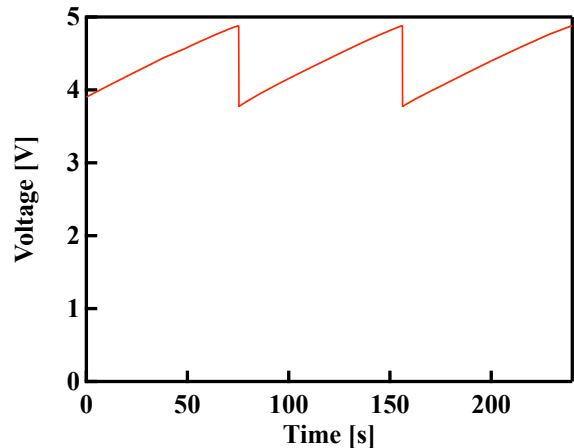


Figure 10. Time trace of the capacitor voltage with the charge/discharge cycle for intermittent wireless transmission.

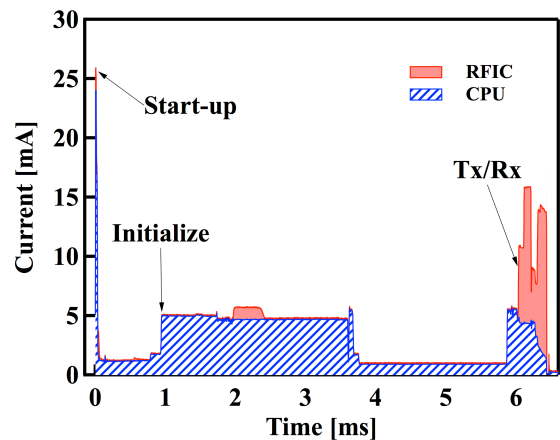


Figure 11. Time trace of the current consumption of the CPU and the RFIC.

a voltage regulator (TPS79930, Texas Instruments), and constant voltage of 3 V is supplied to the CPU and the RFIC. After initialization, temperature data measured with a thermistor are sent via 2.4 GHz RF. For the AC power output of  $5.1 \mu\text{W}$  at the matched impedance, the wireless system is operated intermittently with a period of 80.6 s, showing the feasibility of the present configuration for battery-less sensor network nodes (Fig. 10).

Current consumption of the system is examined in detail. As shown in Fig. 11, after sharp current peak appears for waking-up the CPU, relatively-large current is required for the initialization of CPU. Then,

wireless data transmission at 2.4 GHz is made with the RFIC. The whole process is finished within 6.5 ms. Finally, CPU is shut down, and the regulator is turned off, which restarts charging the capacitor.

In the present device, the energy stored in the capacitor is 29 % of the AC power output. This is due to the impedance mismatch of the circuit. In addition, the energy utilization efficiency defined with the usable energy for the CPU and the RFIC divided by the AC power output is 18 %. Therefore, better impedance matching is crucial to obtain higher efficiency of the power management circuit. In addition, power consumption current of CPU during the settling time is as large as 73 %, which should be minimized by better scheduling of the system.

## CONCLUSION

An early prototype of a battery-less wireless sensor node using a vibration-driven MEMS electret energy harvester has been developed. With the nonlinear parylene springs and CYTOP electrets, maximum power output of 6  $\mu$ W has been obtained at 40 Hz and 1.4 G acceleration. With a pseudo environmental vibration at 1.2  $G_{\text{rms}}$ , mean power output of 3.4  $\mu$ W is also obtained, showing the effectiveness of the nonlinear spring for a broad frequency range operation. By integrating the energy harvester with a power management circuit, a low-power-consumption CPU, and a RF IC, intermittent wireless transmission with an interval of 80.6 s has been realized, although the power utilization efficiency is as low as 18 %.

This work is partially supported through JSPS NEXT Program and the New Energy and Industrial Technology Development Organization (NEDO) of JAPAN. Photomasks are made using the University of Tokyo VLSI Design and Education Center (VDEC)'s 8-inch EB writer F5112+VD01 donated by ADVANTEST Corporation.

## REFERENCES

- [1] S. Roundy, P. K. Wright, and J. Rabaey, "A study of low level vibrations as a power source for wireless sensor nodes," *Comp. Commu.*, Vol. 26, pp.1131-1144, (2003).
- [2] S. P. Beeby, M. J. Tudor, and N. M. White, "Energy harvesting vibration sources for micro systems applications," *Meas. Sci. Technol.*, Vol. 17, pp.175-195, (2006).
- [3] P. D. Mitcheson, E. M. Yeatman, G. K. Rao, A. S. Holmes, and T. C. Green, "Energy harvesting from human and machine motion for wireless electronic devices," *Proc. IEEE*, Vol. 96, pp. 1457-1486, (2008).
- [4] R. J. M. Vullers, R. van Schaijk, I. Doms, C. Van Hoof, and R. Mertens, "Micropower energy harvesting," *Solid-State Electron.*, Vol. 53 pp. 684-693, (2009).
- [5] J. Boland, C. Chao, Y. Suzuki, and Y.-C. Tai, "Micro electret power generator", 16th IEEE Int. Conf. Micro Electro Mechanical Systems (MEMS'03), Kyoto, pp. 538-541, (2003).
- [6] T. Tsutsumino, Y. Suzuki, N. Kasagi, and Y. Sakane, "Seismic power generator using high-performance polymer electret," 19th IEEE Int. Conf. Micro Electro Mechanical Systems (MEMS'06), Istanbul, pp. 98-101, (2006).
- [7] Y. Sakane, Y. Suzuki, and N. Kasagi, "Development of high-performance perfluorinated polymer electret film and its application to micro power generation," *J. Micromech. Microeng.*, Vol. 18, 104011, 6pp, (2008).
- [8] H.-W. Lo, and Y.-C. Tai, "Parylene-based electret power generators," *J. Micromech. Microeng.*, Vol. 18, 104006, 8pp, (2008).
- [9] Y. Naruse, N. Matsubara, K. Mabuchi, M. Izumi, and K. Honma, "Electrostatic micro power generator from low frequency vibration such as human motion," *J. Micromech. Microeng.*, Vol. 19, 094002, 5pp, (2009).
- [10] T. Masaki, K. Sakurai, T. Yokoyama, M. Ikuta, M. Doi, T. Seki, and M. Oba, "Power output enhancement of vibration-driven electret generator using concave electrodes," 10th Int. Workshop on Micro and Nanotechnology for Power Generation and Energy Conversion Applications (PowerMEMS 2010), Leuven, pp. 57-60 (2010).
- [11] Y. Suzuki, "Recent progress in MEMS electret generator for energy harvesting," *IEEJ Trans. Electr. Electr. Eng.*, Vol. 6, No. 2, pp. 101-111 (2011).
- [12] K. Kashiwagi, K. Okano, Y. Morizawa, and Y. Suzuki, "Nano-cluster-enhanced high-performance perfluoro-polymer electrets for micro power generation," 10th Int. Workshop on Micro and Nanotechnology for Power Generation and Energy Conversion Applications (PowerMEMS 2010), Leuven, pp. 169-172 (2010).
- [13] Y. Suzuki, and Y.-C. Tai, "Micromachined high-aspect-ratio parylene spring and its application to low-frequency accelerometers," *J. Micro- electromech. Syst.*, Vol. 15, No. 5, pp. 1364-1370 (2006).
- [14] Y. Suzuki, D. Miki, M. Edamoto, and M. Honzumi, "A MEMS electret generator with electrostatic levitation for vibration-driven energy harvesting applications," *J. Micromech. Microeng.*, Vol. 20, Issue. 10, No. 104002, 8pp, (2010).
- [15] D. Miki, M. Honzumi, Y. Suzuki, and N. Kasagi, "Large-amplitude MEMS electret generator with nonlinear spring," 23rd IEEE Int. Conf. Micro Electro Mechanical Systems (MEMS2010), Hong Kong, China, pp.176-179, (2010).